Pattern and wave number selection in magnetic fluids

René Friedrichs and Andreas Engel
FNW/ITP, Otto-von-Guericke-Universität, Postfach 4120, D-39016 Magdeburg, Germany
(Received 1 February 2001; published 20 July 2001)

The formation of patterns of peaks on the free surface of a magnetic fluid subject to a magnetic field normal to the undisturbed interface is investigated theoretically. The relative stability of ridge, square, and hexagon planforms is studied using a perturbative energy minimization procedure. Extending previous studies the finite depth of the fluid layer is taken into account. Moreover, adding the wave number modulus k to the set of variational parameters also the wave number selection problem is addressed. The results are compared with previous investigations and recent experimental findings.

DOI: 10.1103/PhysRevE.64.021406 PACS number(s): 47.20.Ma, 47.54.+r, 75.50.Mm

I. INTRODUCTION

When a magnetic fluid layer is subjected to a vertically oriented and uniform magnetic field, above a critical value of the field strength a hexagonal pattern of peaks appears on the surface of the liquid. This Rosensweig or normal field instability was first observed by Cowley and Rosensweig in 1967 [1,2]. Further increase of the magnetic field up to a second threshold gives rise to a transition from the hexagonal to a square planform [3,4].

The arrangement of peaks resulting from the Rosensweig instability into patterns of different geometry is just one particular example from an impressive variety of pattern formation in physical systems [5]. It is well known that although the instability threshold itself can be obtained from a linearized version of the underlying equations, the pattern selection problem requires the inclusion of nonlinear terms. A standard procedure to probe the nonlinear regime perturbatively is by means of amplitude equations [6,5].

However, unlike many other examples of pattern forming physical systems discussed in the literature, the surface profile of a magnetic fluid in a static magnetic field is an equilibrium structure. Accordingly, the relative stability of planforms and possible transitions between different patterns can be investigated theoretically by studying the appropriate thermodynamical potential. Still the problem is a complicated nonlinear task since the local magnetic field determining the surface profile in turn depends on the surface deflection via boundary conditions. As a consequence the variational minimization of the thermodynamic potential in the surface profile cannot be accomplished exactly and one has to resort to approximate procedures applicable in the experimentally relevant situation of slightly overcritical magnetic fields.

In classical investigations along these lines Gailitis [7] and Kuznetsov and Spektor [8] analyzed the stability of the different patterns of the Rosensweig instability by means of an energy minimization principle. These as well as related investigations using methods of functional analysis [9,10] or a generalized Swift-Hohenberg equation [11,12] were confined to fluid layers of infinite depth.

On the other hand, experimental investigations are usually done with rather thin fluid layers and the effects of finite thickness on the *linear* regime have been studied recently in great detail. For example, the dispersion relation of surface waves on a magnetic fluid layer of arbitrary thickness was determined in Ref. [13] and the influence of viscosity on the linear dynamics was elucidated in Ref. [14]. Taking advantage of the dependence of the threshold of instability and the wavelength of the most unstable mode on the thickness of the fluid layer in a clever way, it is, e.g., possible to measure both the normal and the anomalous dispersion branch of surface waves on magnetic fluids [15].

In the present paper we complement these investigations by a thorough study of the weakly nonlinear regime of the Rosensweig instability slightly above the critical magnetic field for a magnetic fluid of arbitrary depth. Taking the limit of infinite layer thickness we also critically discuss the classical findings obtained in Refs. [7] and [8]. Moreover, we are able to quantify the restriction to sufficiently small susceptibilities χ of the fluids which was always used in previous studies.

Our method of investigation is a generalization of the variational minimization of an energy functional already used in Refs. [7] and [8]. Near the instability this functional may be written as a power series in the amplitude of the surface deflection and the minimization can be performed explicitly. Moreover, our approach allows the theoretical investigation of the wave number selection problem addressed also in recent experiments [4]. Including the wave number k into the set of variational parameters we determine the dependence of the wave number of the patterns on the magnetic field and investigate the influence of a varying wave number on the stability of hexagons and squares. Therefore by a slight extension of our method we are able to study questions which are not easily accessible to other nonlinear methods, as, e.g., amplitude equations.

The paper is organized as follows. In Sec. II the basic equations are collected and transformed into a form suitable for the calculation of the energy. In Sec. III a perturbation ansatz for the surface deflection is put forward and the important issue of its consistency and region of validity is discussed. Section IV is devoted to the comparison of our findings with the classical results of pattern selection in a fluid with infinite depth. Subsequently in Sec. V we consider a magnetic fluid layer with arbitrary thickness and analyze the effects of the finite depth on the stability of the patterns. In Sec. VI we address the wave number selection problem. Fi-

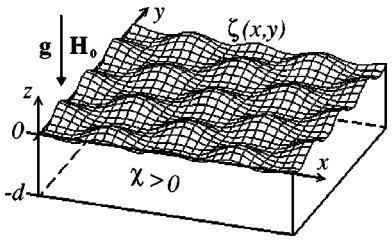

FIG. 1. Schematic plot of a magnetic fluid layer with infinite horizontal extension in an external magnetic field $\mathbf{H}_0$ parallel to the gravitational acceleration **g**. We investigate the pattern formation on the free surface $z=\zeta(x,y)$ for arbitrary depth d of the magnetic fluid with susceptibility $\chi>0$.

nally Sec. VII contains a summary and compares our findings with recent experimental results.

II. BASIC EQUATIONS

We consider the situation sketched in Fig. 1. A horizontally unbounded magnetic fluid layer is subjected to an external magnetic field $\mathbf{H}_0$ which in the absence of any magnetic permeable material is of the form $\mathbf{H}_0(x,y,z)=-H_0\mathbf{e}_z$. The incompressible magnetic fluid of density ρ, surface tension σ, and susceptibility χ is bounded from below at $z=-d$ by an impermeable material and has a free surface described by $z=\zeta(x,y)$ with the magnetically impermeable air above. The gravitational acceleration $\mathbf{g}=-g\mathbf{e}_z$ acts parallel to the z axis. Our aim is to determine which static profile $\zeta(x,y)$ develops for a magnetic field $\mathbf{H}_0$ strong enough to destabilize the flat surface $\zeta(x,y)=0$.

Stable configurations of the magnetic fluid surface with infinite horizontal extension are given by minima of the thermodynamic potential per unit area in the x-y plane

$$f[\zeta(x,y)]=\left\langle \frac{\rho g}{2}\zeta^2(x,y)-\frac{\mu_0}{2}\int_{-d}^{\zeta(x,y)}dz\mathbf{H}_0\chi\mathbf{H}(x,y,z) + \sigma\sqrt{1+(\partial_x\zeta(x,y))^2+(\partial_y\zeta(x,y))^2}\right\rangle. \quad (1)$$

Here μ_0 is the permeability of free space, $\mathbf{H}(x,y,z)$ is the magnetic field in the presence of the magnetic fluid, and the brackets denote the average over the x-y plane defined by

$$\langle F(x,y)\rangle := \lim_{L\to\infty}\frac{1}{4L^2}\int_{-L}^{L}dx\int_{-L}^{L}dyF(x,y). \quad (2)$$

The three terms on the right-hand side of Eq. (1) describe the hydrostatic energy, the magnetic energy [16], and the surface energy, respectively. Note that both the hydrostatic and the surface energy increase when the interface profile starts to deviate from the flat reference state, whereas the magnetic energy decreases. For sufficiently large $\mathbf{H}_0$ this gives rise to the normal field or Rosensweig instability [1,2].

The magnetic fields **B** and **H** are determined by the static Maxwell equations,

$$\nabla\cdot\mathbf{B}=0 \quad \text{and} \quad \nabla\times\mathbf{H}=0, \quad (3)$$

together with the boundary conditions,

$$\lim_{z\to\pm\infty}\mathbf{H}(x,y,z)=-H_0\mathbf{e}_z, \quad (4)$$

$$[(\mathbf{B}_a-\mathbf{B}_{ff})\cdot\mathbf{n}]|_{z=\zeta}=0 \quad \text{and} \quad [(\mathbf{H}_a-\mathbf{H}_{ff})\times\mathbf{n}]|_{z=\zeta}=0, \quad (5)$$

$$[(\mathbf{B}_{ff}-\mathbf{B}_b)\cdot\mathbf{e}_z]|_{z=-d}=0 \quad \text{and} \quad [(\mathbf{H}_{ff}-\mathbf{H}_b)\times\mathbf{e}_z]|_{z=-d}=0, \quad (6)$$

where **n** denotes the normal vector on the surface $\zeta(x,y)$ and the respective subscripts indicate the fields above, in, and below the magnetic fluid. The minimization problem for the thermodynamic potential becomes nontrivial since the magnetic field $\mathbf{H}(x,y,z)$ depends on the profile $\zeta(x,y)$ of the surface.

Throughout the paper we will assume the linear relation

$$\mathbf{B}=\mu_0(1+\chi)\mathbf{H} \quad (7)$$

between the magnetic induction and the magnetic field. For the experimentally relevant magnetic fluids and fields [4] this approximation deviates about 5% from the exact relation between **B** and **H**.

It is convenient to introduce a scalar magnetic potential $\psi(x,y,z)$ defined by

$$\mathbf{H}=-\nabla\psi, \quad (8)$$

which by Eq. (3) has to satisfy the Laplace equation

$$\Delta\psi=0. \quad (9)$$

The two characteristic scales of the problem are the critical wave number at the onset of the instability,

$$k_{c,\infty}=\sqrt{\frac{\rho g}{\sigma}}, \quad (10)$$

for a magnetic fluid with infinite depth $d\to\infty$ and the corresponding critical magnetic field,

$$H_{c,\infty}=\sqrt{\frac{(1+\chi)(2+\chi)2\sqrt{\rho g\sigma}}{\chi^2\mu_0}}, \quad (11)$$

which were first derived in Ref. [1] from a linear stability analysis. Henceforth we therefore measure all lengths in units of the capillary length $k_{c,\infty}^{-1}$, all wave numbers in units of the critical wave number $k_{c,\infty}$, the magnetic field $\mathbf{H}_0$ in units of the critical value $H_{c,\infty}$, the scalar magnetic potential ψ in units of $H_{c,\infty}/k_{c,\infty}$, and energies per unit area in units of σ. Moreover, it is convenient to introduce the following rescaled magnetic potentials in the space above, in, and below the magnetic fluid, respectively:

$$\psi_a := \psi\frac{(2+\chi)}{H_0\chi}, \quad (12)$$

$$\psi_{ff} := \psi\frac{(1+\chi)(2+\chi)}{H_0\chi}, \quad (13)$$

$$\psi_b := \psi \frac{(2+\chi)}{H_0 \chi}. \tag{14}$$

Each of these potentials has to fulfill the Laplace Eq. (9). Using the abbreviation

$$\eta := \frac{\chi}{2+\chi}. \tag{15}$$

the asymptotic form of the magnetic field for $|z| \to \infty$ as specified by Eq. (4) gives rise to the requirements

$$\lim_{z \to +\infty} \partial_z \psi_a(x,y,z) = \frac{1}{\eta} = \lim_{z \to -\infty} \partial_z \psi_b(x,y,z) \tag{16}$$

for the magnetic potentials. Moreover the boundary conditions (5) and (6) for the magnetic fields translate into the following boundary conditions for the potentials:

$$[\partial_x \psi_a - \partial_x \psi_{ff}]|_{z=\zeta} \partial_x \zeta + [\partial_y \psi_a - \partial_y \psi_{ff}]|_{z=\zeta} \partial_y \zeta - [\partial_z \psi_a - \partial_z \psi_{ff}]|_{z=\zeta} = 0, \tag{17}$$

$$\frac{1+\eta}{1-\eta} \psi_a \Big|_{z=\zeta} - \psi_{ff}|_{z=\zeta} = 0, \tag{18}$$

$$[\partial_z \psi_{ff} - \partial_z \psi_b]|_{z=-d} = 0, \tag{19}$$

$$\psi_{ff}|_{z=-d} - \frac{1+\eta}{1-\eta} \psi_b \Big|_{z=-d} = 0. \tag{20}$$

Using Eqs. (8) and (13) and exploiting the fact that $\mathbf{H}_0$ is parallel to the z axis, we finally get the energy f as functional of the surface deflection $\zeta = \zeta(x,y)$ in the form

$$f[\zeta] = \left\langle \frac{\zeta^2}{2} - H_0^2 (\psi_{ff}|_{z=\zeta} - \psi_{ff}|_{z=-d}) + \sqrt{1 + (\partial_x \zeta)^2 + (\partial_y \zeta)^2} \right\rangle. \tag{21}$$

As stated above, the main problem, rendering a straightforward minimization of f in $\zeta(x,y)$ impossible, is the rather implicit dependence of the potential $\psi_{ff}(x,y,z)$ on the surface deflection $\zeta(x,y)$ specified by the boundary conditions (17) and (18).

III. THE PERTURBATION *ANSATZ*

The variational problem for the energy functional posed in the last paragraph can in general not be solved exactly. In order to make analytic progress, we restrict ourselves to the vicinity of the critical magnetic field and assume that the amplitude of the surface deflection is still small. It is then possible to expand the energy in this amplitude and to retain only the first terms. In this paper we will consider an expansion of the energy up to fourth order in the amplitude. The applicability of this approach will be critically discussed below.

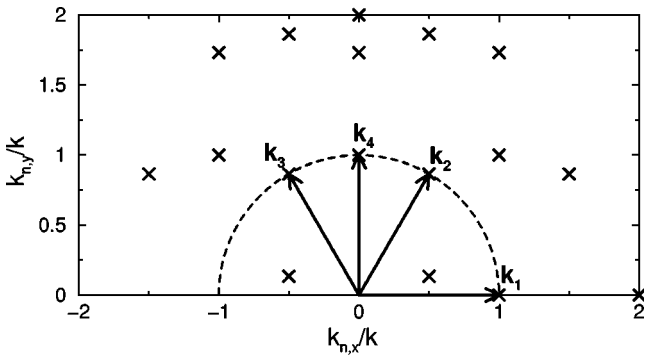

FIG. 2. Wave vectors $\mathbf{k}_1$ to $\mathbf{k}_4$ of the four main modes in the perturbation ansatz (22) (arrows). $\mathbf{k}_4$ is perpendicular to $\mathbf{k}_1$ and the angle between $\mathbf{k}_1$ and $\mathbf{k}_2$ or $\mathbf{k}_2$ and $\mathbf{k}_3$ is $\pi/3$. The end points of the wave vectors of the higher harmonics are represented by crosses. Each of these wave vectors is the sum or difference of two of the main wave vectors.

Generalizing the perturbation expansions used in Refs. [7], [8], [19], and [23] for the one-dimensional variant of the Rosensweig instability, we write the surface profile in the form

$$\zeta(x,y) = \sum_{n=1}^{4} A_n \cos(\mathbf{k}_n \cdot \mathbf{r}) + \sum_{n=5}^{17} B_n \cos(\mathbf{k}_n \cdot \mathbf{r}), \tag{22}$$

where $\mathbf{r} = (x,y)$ and $\mathbf{k} = (k_x, k_y)$ are two-dimensional vectors. The terms with $n = 1, \ldots, 4$ constitute the main modes. Their corresponding wave vectors $\mathbf{k}_1$ to $\mathbf{k}_4$ have all the same modulus k whereas their mutual orientation is chosen such that the *Ansatz* allows the description of ridges (e.g., $A_1 = A$, $A_2 = A_3 = A_4 = 0$), squares (e.g., $A_1 = A_4 = A$, $A_2 = A_3 = 0$), and hexagons (e.g., $A_1 = A_2 = A_3 = A$, $A_4 = 0$) (see Fig. 2).

The terms with $n = 5, \ldots, 17$ are higher harmonics with wave vectors $\mathbf{k}_5$ to $\mathbf{k}_{17}$ being linear combinations of two wave vectors of the main modes and amplitudes B_n of order $O(A^2)$. These terms are needed to satisfy the minimum conditions for the energy functional to the required order $O(A^3)$. The intuitive meaning of this fact is that reliable results on the relative stability of different planforms requires some information on the deviation of the nonlinear surface profile from the simple cosine shape describing the linear instability. On the other hand, there is no need to include even higher harmonics in the ansatz (22) since the corresponding contributions would average to zero in the x-y integrations in the definition (21) of the energy functional. In conclusion the chosen *Ansatz* is the only consistent perturbation ansatz for the energy which includes terms up to fourth order in the amplitude of the surface deflection. The values of the amplitudes $A_1, \ldots, A_4$ and $B_5, \ldots, B_{17}$ as well as the wave vector modulus k of the main modes are the free parameters which may be used to minimize the energy. In particular the possible minimization in k is a special advantage of our approach since it allows an analysis of the nonlinear wave vector selection problem not easily accessible to other approaches.

Because of the boundary conditions at the surface of the fluid the magnetic potential ψ must have a similar dependence on x and y as $\zeta(x,y)$. The *Ansätze*

$$\psi_{\mathrm{a}}=\frac{z}{\eta}+\sum_{n=0}^{17} u_n e^{-|\mathbf{k}_n|z}\cos(\mathbf{k}_n\cdot\mathbf{r}),$$

$$\psi_{\mathrm{ff}}=\frac{z}{\eta}+\sum_{n=1}^{17}\left[v_n^{+}e^{|\mathbf{k}_n|z}+v_n^{-}e^{-|\mathbf{k}_n|z}\right]\cos(\mathbf{k}_n\cdot\mathbf{r}),$$

$$\psi_{\mathrm{b}}=\frac{z}{\eta}+\frac{2d}{1+\eta}+\sum_{n=0}^{17} w_n e^{|\mathbf{k}_n|z}\cos(\mathbf{k}_n\cdot\mathbf{r}), \tag{23}$$

fulfill the Laplace Eq. (9) and the asymptotic boundary conditions (16). Omitting the mode $\mathbf{k}_0:=(0,0)$ in the potential ψ_{ff} fixes the free constant of the potential ψ. Plugging Eq. (23) into the four remaining boundary conditions Eqs. (17)–(20) we can determine the parameters u_n, v_n^{+}, v_n^{-}, and w_n as functions of the surface deflection amplitudes by expanding the equations up to third order in the A_n. The resulting expressions specify the dependence of the magnetic field on the surface profile which is then used to calculate the energy f using Eq. (21) up to fourth order in the amplitudes A_n. The resulting dependence of f on the higher order amplitudes B_n is simple and the minimization in the B_n can be performed explicitly. Subtracting from the resulting expression the reference value of the energy for a flat interface we finally arrive at

$$f_d(\{A_n\},k):=f(\{A_n\},k)-f(\zeta=0) \tag{24}$$

$$\begin{aligned}=&-\frac{1}{2}l(\epsilon,k)[A_1^2+A_2^2+A_3^2+A_4^2]\\&-\gamma(\epsilon,k)[A_1A_2A_3]+\frac{1}{4}g(\epsilon,k)[A_1^4+A_2^4\\&+A_3^4+A_4^4]+\frac{1}{2}g_h(\epsilon,k)[A_1^2A_2^2+A_2^2A_3^2\\&+A_3^2A_1^2]+\frac{1}{2}g_t(\epsilon,k)[A_2^2A_4^2+A_3^2A_4^2]\\&+\frac{1}{2}g_n(\epsilon,k)[A_1^2A_4^2]+O(A^5).\end{aligned} \tag{25}$$

This expression gives the energy of a magnetic fluid layer of depth d with surface profile $\zeta(x,y)$ as specified by Eq. (22) at arbitrary strength of the external field H_0 up to fourth order in the deflection amplitudes A_n. The dependence on H_0 is expressed via the supercriticality parameter

$$\epsilon=\frac{H_0^2}{H_{c,d}^2}-1. \tag{26}$$

The function $l(\epsilon,k)$ is given by

$$l(\epsilon,k)=-\frac{1}{2}+(1+\epsilon)H_{c,d}^2\frac{1-e^{-2kd}\eta}{1-e^{-2kd}\eta^2}k-\frac{1}{2}k^2. \tag{27}$$

It fixes the critical wave number $k_{c,d}$ for the onset of the instability and the corresponding critical magnetic field $H_{c,d}$ for a magnetic fluid with *finite* depth d via the conditions

$$l(\epsilon=0)|_{k=k_{c,d}}=0 \tag{28a}$$

and

$$\frac{\partial l(\epsilon=0)}{\partial k}|_{k=k_{c,d}}=0. \tag{28b}$$

Determining the minima of f with respect to the amplitudes A_n, one finds that $\epsilon\to 0$ with $A_n\to 0$ as expected: the external field will be near to its critical value if the *equilibrium* values of the amplitudes A_n are small. For ridges and squares the explicit scaling is $\epsilon\sim A^2$ for $A\to 0$, in the case of hexagons one finds $\epsilon\sim -A$ for small A. This in turn implies that to the desired order $O(A^4)$ of the expansion of f in the amplitudes A_n only the ϵ dependence of l and γ has to be retained. The exact form of these dependencies is $l(\epsilon,k)=l(0,k)+\epsilon\partial l(\epsilon,k)/\partial\epsilon$ and $\gamma(\epsilon,k)=(1+\epsilon)\gamma(k)$. In this way we arrive at our main result for the energy $f_d(\{A_n\},k)$ of the surface deflection which describes the equilibrium configurations consistently up to fourth order in the amplitudes A_n:

$$\begin{aligned}f_d(\{A_n\},k)=&-\frac{1}{2}l(\epsilon,k)[A_1^2+A_2^2+A_3^2+A_4^2]-(1+\epsilon)\gamma(k)\\&\times[A_1A_2A_3]+\frac{1}{4}g(k)[A_1^4+A_2^4+A_3^4+A_4^4]\\&+\frac{1}{2}g_h(k)[A_1^2A_2^2+A_2^2A_3^2+A_3^2A_1^2]+\frac{1}{2}g_t(k)\\&\times[A_2^2A_4^2+A_3^2A_4^2]+\frac{1}{2}g_n(k)[A_1^2A_4^2]+O(A^5).\end{aligned} \tag{29}$$

The explicit expressions for the various coefficients in Eq. (29) are rather long. We therefore display their form here only for the comparatively simple situation of a fluid of infinite depth, $d\to\infty$:

$$\gamma_\infty(k)=\frac{3}{4}\eta k^2, \tag{30a}$$

$$g_\infty(k)=\frac{1}{16}k^3(8-3k)-\frac{k^4\eta^2}{1-4k+4k^2}, \tag{30b}$$

$$\begin{aligned}g_{h,\infty}(k)=&\frac{1}{4}k^3\left(11\eta^2-7\eta^2\sqrt{3}+3\sqrt{3}-\frac{3}{4}k-3\right)\\&-\frac{3}{8}\frac{k^4\eta^2(19-8\sqrt{3})}{1-2\sqrt{3}k+3k^2},\end{aligned} \tag{30c}$$

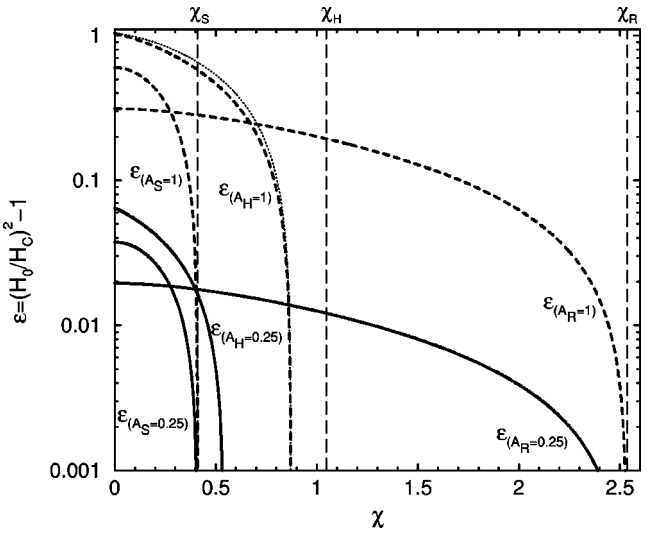

FIG. 3. Lines separating regions in the χ-ϵ plane in which the amplitudes of ridges A_R, squares A_S, and hexagons A_H, are smaller than 0.25 (full lines) or smaller than 1 (dashed lines). The thin dotted line represents the results given in Ref. [7]. For susceptibilities larger than the critical values χ_R, χ_S, and χ_H the amplitudes diverge in the considered approximation (22).

$$g_{t,\infty}(k)=k^3\left(\frac{3}{4}\sqrt{3}\sqrt{2}-1+4\,\eta^2-\frac{7}{4}\,\eta^2\sqrt{3}\sqrt{2}-\frac{5}{16}k\right)$$
$$-\frac{1}{8}\,\frac{\eta^2k^4(18+\sqrt{3}-4\sqrt{2}-4\sqrt{3}\sqrt{2})}{2-k\sqrt{3}\sqrt{2}+k^2+k\sqrt{2}-\sqrt{3}}$$
$$-\frac{1}{8}\,\frac{\eta^2k^4(18-\sqrt{3}+4\sqrt{2}-4\sqrt{3}\sqrt{2})}{2-k\sqrt{3}\sqrt{2}+k^2-k\sqrt{2}+\sqrt{3}}, \qquad (30d)$$

$$g_{n,\infty}(k)=k^3\left(-\frac{1}{8}k-3\,\eta^2\sqrt{2}-1+4\,\eta^2+\sqrt{2}\right)$$
$$-\frac{k^4\eta^2(9-4\sqrt{2})}{1-2k\sqrt{2}+2k^2}. \qquad (30e)$$

IV. FERROFLUID LAYER WITH INFINITE DEPTH

In this section we consider a magnetic fluid of infinite depth $d\to\infty$ and fix the wave number modulus k at its critical value $k_{c,\infty}=1$. This enables us to compare our findings with the well-known results of previous theoretical investigations.

Possible surface patterns together with their amplitudes are given by stationary points of the energy function $f_\infty(\{A_n\},k=1)$. We will in particular study ridges (''rolls'') given by $A_1=A_R$ with $A_2=A_3=A_4=0$, squares represented by $A_1=A_4=A_S$ with $A_2=A_3=0$, and hexagons described by $A_1=A_2=A_3=A_H$ with $A_4=0$. The last planform is shown in Fig. 1. Using Eqs. (27), (29), and (30) we find for the corresponding amplitudes

$$A_R(\epsilon)=\sqrt{\frac{\epsilon}{g_\infty}}, \qquad (31)$$

$$A_S(\epsilon)=\sqrt{\frac{\epsilon}{g_{n,\infty}+g_\infty}}, \qquad (32)$$

and

$$A_H(\epsilon)=\frac{1}{2}\,\frac{\gamma_\infty(1+\epsilon)+\sqrt{\gamma_\infty^2(1+\epsilon)^2+4\epsilon(2g_{h,\infty}+g_\infty)}}{2g_{h,\infty}+g_\infty}, \qquad (33)$$

respectively. Together with χ also γ is always positive.[1] Hence only up hexagons with a peak instead of a dip in the center are stable.

Our results for the hexagons differ slightly from the classical ones reported in Ref. [7] in which the dependence of the cubic term in Eq. (29) on ϵ is missing. In Refs. [7] and [8] this dependence was omitted because the discussion was restricted to fluids with $\gamma\ll 1$ so that the approximate scaling $\epsilon\sim A^2$ is very similar to the true one $\epsilon\sim-\gamma A+O(A^2)$ and the hysteresis effect of the first-order transition [17,18] small. Otherwise our results coincide with those of Gailitis, in particular using $k=k_{c,\infty}=1$ in Eq. (30) the respective expressions found in Ref. [7] are reproduced. The investigations of Kuznetzov and Spektor [8] were restricted to first order in η and are contained in both our results and those of Gailitis.

Before addressing the relative stability of the different planforms introduced above it is important to characterize the domain of validity of our central expression (29) for the energy. Being a perturbative result the corresponding amplitudes A_n must not be too large. Figure 3 gives a quantitative impression of what that means by displaying lines in the $\chi-\epsilon$ plane corresponding to fixed values of the amplitudes of different patterns. It is in particular important to realize that for sufficiently large values of the susceptibility χ the fourth order coefficients in the energy functional may change sign. The corresponding patterns than appear through a backward bifurcation [10]. At the same time *higher order* terms (i.e., sixth or higher order in the amplitudes A_n) in the energy are necessary to saturate the instability. The concrete values of χ for the planforms considered are $\chi_R\approx 2.54$ (g_∞ becomes negative), $\chi_S\approx 0.41$ ($g_{n,\infty}+g_\infty$ becomes negative), and $\chi_H\approx 1.05$ ($2g_{h,\infty}+g_\infty$ becomes negative). Beyond these values of χ our ansatz (22) is unable to describe the arising pattern. The value of χ_R was first calculated in Ref. [19].

Keeping this limitation of our approach in mind we have investigated the pattern selection problem by studying the character of the extremum of the energy functional (29) at the ridge, square, and hexagon solutions given in Eqs. (31)–(33). This is rather similar to a linear stability analysis of the fix point solutions of the corresponding amplitude equations [20]. The results are as follows: Ridges are never stable, since $g_{n,\infty}<g_\infty$ always. We have always $g_\infty+g_{n,\infty}<g_{h,\infty}+g_{t,\infty}$ and $g_{n,\infty}<g_\infty$. Hence (for $\chi<\chi_S$) squares are stable if

[1]This holds true also in the case of a finite layer depth d.

$$\epsilon > \epsilon_S = \frac{[g_\infty + g_{n,\infty} - g_{h,\infty} - g_{t,\infty} + \sqrt{(g_\infty + g_{n,\infty} - g_{h,\infty} - g_{t,\infty})^2 - 4\gamma_\infty^2 (g_\infty + g_{n,\infty})}]^2}{4\gamma_\infty^2 (g_\infty + g_{n,\infty})}.$$

In order for hexagons to be stable (for $\chi < \chi_H$) the following three conditions have to be fulfilled:

(i) $$\epsilon > \epsilon_F = \frac{[\gamma_\infty^2 + 2g_{h,\infty} + g_\infty - \sqrt{(\gamma_\infty^2 + 2g_{h,\infty} + g_\infty)(2g_{h,\infty} + g_\infty)}][2g_{h,\infty} + g_\infty - \sqrt{(\gamma_\infty^2 + 2g_{h,\infty} + g_\infty)(2g_{h,\infty} + g_\infty)}]}{\gamma_\infty^2 \sqrt{(\gamma_\infty^2 + 2g_{h,\infty} + g_\infty)(2g_{h,\infty} + g_\infty)}};$$

(ii) either $$\epsilon < \epsilon_H = \frac{\gamma_\infty^2 (g_{h,\infty} + 2g_\infty)}{(\gamma_\infty^2 + g_{h,\infty} - g_\infty)(g_{h,\infty} - g_\infty)}$$ or $g_{h,\infty} < g_\infty$;

(iii) either $$\epsilon < \epsilon_h = \frac{\gamma_\infty^2 (g_{n,\infty} + 2g_{t,\infty})}{(\gamma_\infty^2 + 2g_{h,\infty} + g_\infty - 2g_{t,\infty} - g_{n,\infty})(2g_{h,\infty} + g_\infty - 2g_{t,\infty} - g_{n,\infty})}$$ or $2g_{h,\infty} + g_\infty < 2g_{t,\infty} + g_{n,\infty}$.

These results are displayed in Fig. 4. For regions in which two different patterns are stable, i.e., in which different local minima of the energy exist, we have also determined the respective Maxwell values of ϵ at which these minima have the same value. For $\epsilon = \epsilon_{HS}$ the energy of the hexagon pattern is equal to the energy of the square pattern, for $\epsilon = \epsilon_{HF}$ it is equal to the energy of the flat surface.

For all susceptibilities either the relation $g_{h,\infty} < g_\infty$ or the relation $2g_{h,\infty} + g_\infty < 2g_{t,\infty} + g_{n,\infty}$ is violated and consequently hexagons always become unstable for sufficiently large ϵ.

Of particular importance is the line denoted by ϵ_h. For $\epsilon > \epsilon_h$ the hexagon pattern is unstable to squares which in turn for $\chi > \chi_S$ are not saturated by the fourth order term in the energy. In that case within our perturbation ansatz we are not able to predict which pattern will show up. For $\chi > \chi_O \approx 0.56$ this transition occurs right at onset and our analysis of hexagons is therefore restricted to $\chi < 0.56$. This stability criterion for hexagons was to our knowledge not discussed in the literature before. It was not found by Silber and Knobloch [10], since with their approach the relative stability between hexagons and squares could not be determined. It was also missed by Gailitis [7] and by Kuznetsov and Spektor [8] since they considered only the case $\chi \ll 1$.

V. FERROFLUID LAYER WITH ARBITRARY THICKNESS

The aim of this section is to investigate how the finite depth d of a magnetic fluid layer affects the pattern selection. Only magnetic fluids with relatively small susceptibilities $\chi < \chi_S$ will be considered in order not to leave the region of applicability of our perturbation approach (see the discussion above).

From the linear stability analysis [1,21] it is well known that a thin layer retards the onset of the instability and shifts the wave number of the unstable mode to larger values. The dependence of the critical magnetic field $H_{c,d}$ and of the corresponding critical wave number $k_{c,d}$ on the layer thickness d can be determined from Eqs. (28). It is shown in Fig. 5. If the depth d of the fluid is larger then the critical wavelength at infinite depth $\lambda_{c,\infty} = 2\pi/k_{c,\infty}$, which is typically of the order of 10 mm, the finite thickness of the layer can be ignored. Even if the layer is very thin, the parameters characterizing the linear instability of the flat surface are modified only within a few percent for fluids with small susceptibilities.

To start with the nonlinear analysis we have first to determine the dependence on d of the critical values χ_R, χ_S, and χ_H beyond which higher order terms in the energy functional are necessary. The corresponding results are shown in Fig. 6. All values of the critical susceptibilities get eventually

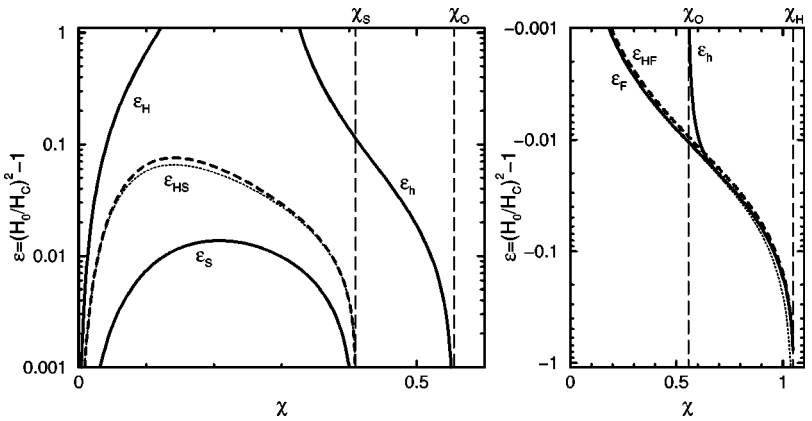

FIG. 4. Limits of the stability regions (solid lines) and Maxwell points (dashed lines) in the χ-ϵ plane. The left figure refers to positive values of ϵ, the right to the subcritical region $\epsilon < 0$. Squares are stable if $\epsilon > \epsilon_S$. Hexagons are stable if $\epsilon < \epsilon_H$, $\epsilon < \epsilon_h$ and $\epsilon > \epsilon_F$. The two thin dotted lines illustrate exemplarily the corresponding findings if the dependence of the cubic term in Eq. (29) on ϵ is neglected.

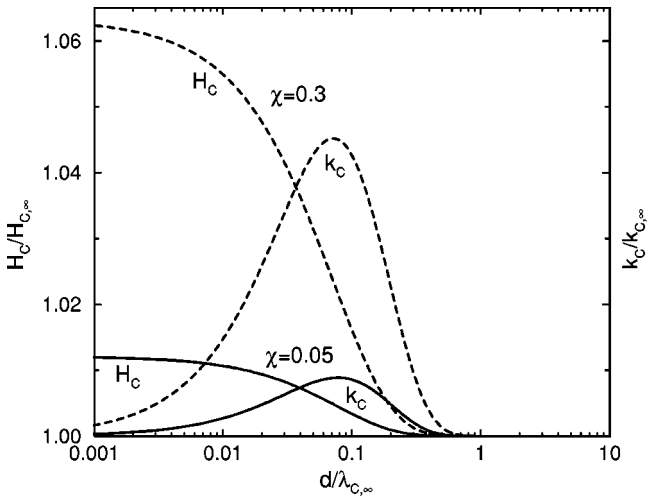

FIG. 5. Critical magnetic field H_c and corresponding critical wave number k_c as functions of the layer thickness d in units of $\lambda_{c,\infty}$, where $\lambda_{c,\infty}$ is the critical wavelength for the layer with infinite thickness. Both critical values are altered less than 2% for a fluid with $\chi=0.05$ (solid lines) and less than 7% for a fluid with $\chi=0.30$ (dashed lines).

smaller if the layer depth decreases. They do not cross each other such that χ_S is the smallest one for all values of d. We have included the result for ridges also although these are unstable in the setup of Fig. 1 for all d and χ. However, ridges can be stabilized by an additional magnetic field tangential to the undisturbed surface [22] and therefore our results give first informations on the behavior in this modified experimental setup.

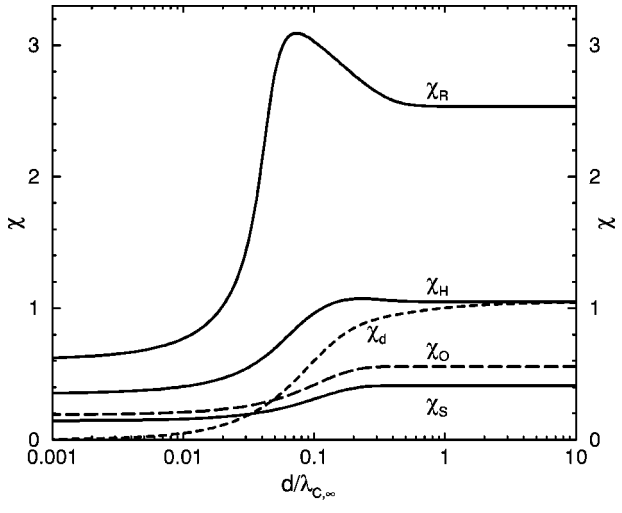

FIG. 6. The critical susceptibilities χ_R, χ_S, and χ_H beyond which higher order terms are necessary in the energy functional in order to describe the respective pattern consistently as function of the layer thickness d. Also included are the values for χ_O beyond which hexagons are unstable to subcritical squares introduced in Sec. IV and $\chi>\chi_d(d)$ for which the pattern amplitude at onset already exceeds the layer thickness. In both cases our theoretical model ceases to be applicable.

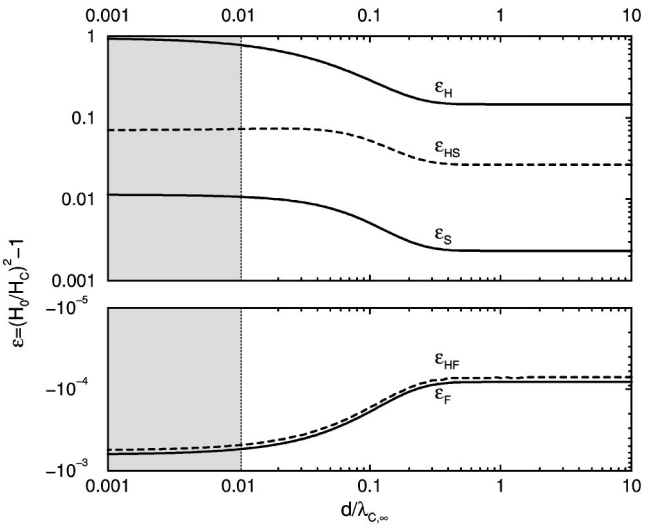

FIG. 7. Limits of the stability regions (solid lines) and Maxwell points (dashed lines) as functions of the layer thickness d for a magnetic fluid with $\chi=0.05$. Ridges are always unstable, squares are stable for $\epsilon>\epsilon_S$, and hexagons are stable for $\epsilon_F<\epsilon<\epsilon_H$. In the gray region the instability results in the formation of dry spots right at onset, so that our theory no longer applies. The lower part of the figure describes the subcritical region.

For very shallow layers the amplitude of the arising pattern may become larger than the layer depth already at onset. As a consequence the magnetic fluid layer disintegrates into unconnected regions and ''dry spots'' occur. This topological change is outside our theoretical analysis. The corresponding value of χ denoted by χ_d is also shown in Fig. 6. As expected it becomes the smallest of all critical χ values for $d\rightarrow 0$.

In order to investigate the stability of the patterns arising on a layer with finite thickness we can perform basically the same analysis as in the previous section. We just have to fix the wave number k to its critical value $k_{c,d}$ corresponding to the given thickness d and to use the appropriate value for $H_{c,d}$ in the function $l(\epsilon,k=k_{c,d})$ [see Eq. (27)]. Moreover, we have to take into account the dependence of the coefficients γ, g, g_h, g_t, and g_n on the depth d. In this way we can finally determine for any given depth d the stability regions of the different patterns by means of the corresponding energy function $f(\{A_n\},k=k_{c,d})$ as given by Eq. (29).

The results for the various stability boundaries and corresponding Maxwell points for a fluid with susceptibility $\chi=0.05$ are shown in Fig. 7. All the critical values of ϵ at which transitions between different planforms arise increase in absolute value with decreasing layer thickness d. Simultaneously the hysteretic behavior becomes more pronounced. As in the linear analysis we find that the effects of finite depth can be neglected, as long as the fluid layer is thicker then the critical wavelength $\lambda_{c,\infty}$. However, for a thin layer the stability of the hexagons and squares is changed noticeably. For instance the value of ϵ_H at which the transition from hexagons to squares takes place may increase by a factor of 3 implying an increase of the magnetic field of about 10%. As discussed above for very thin layers our theory is no longer applicable since the dips of the hexagonal pattern at

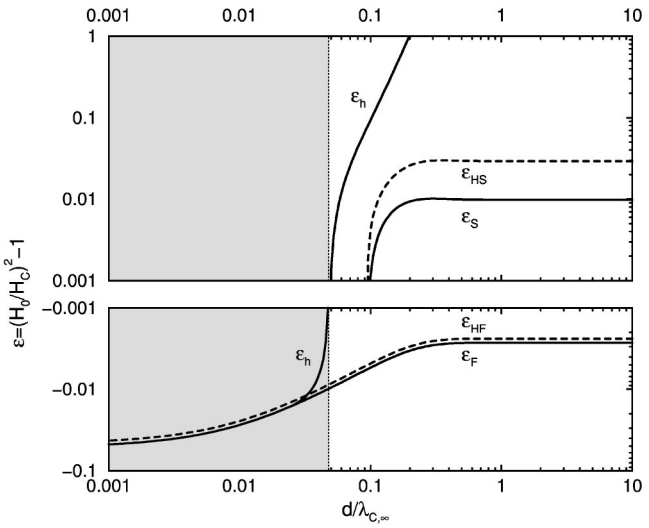

FIG. 8. The same as Fig. 7 for a magnetic fluid with $\chi=0.30$. With decreasing depth d of the layer both $\chi_S(d)$ and $\chi_O(d)$ become smaller than the susceptibility of the fluid and higher order terms in the energy would be needed to determine the pattern stability.

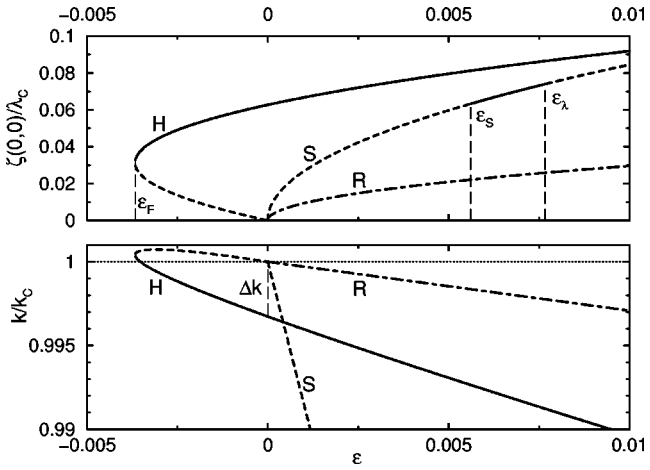

FIG. 9. Surface deflection $\zeta(0, 0)$ at the cusps of the pattern and emerging wave number k in dependence on the supercriticality parameter ϵ. For a fluid with $\chi=0.35$ squares are only stable in the region $\epsilon_S<\epsilon<\epsilon_\lambda$. Ridges are always unstable.

onset already reach the bottom of the fluid. The corresponding values of d are indicated by the shading in Fig. 7.

Figure 8 displays the analogous results as obtained for a magnetic fluid with the larger susceptibility of $\chi=0.30$. Whereas the situation for $\epsilon<0$ is rather similar to the one shown in Fig. 7, the behavior for positive ϵ is qualitatively different. This is due to the fact that although $\chi_S(d\to\infty)>\chi$ with decreasing depth d both $\chi_S(d)$ and $\chi_O(d)$ eventually become smaller than 0.30 (cf. Fig. 6). This gives rise to the divergencies in the energy discussed above and changes the stability chart accordingly.

VI. WAVE NUMBER SELECTION

In many pattern forming systems the wavelength of the first unstable mode is often a good estimate for the typical length scale of the emerging pattern. If a whole band of modes is unstable the one with maximal growth rate is likely to dominate the arising structure [14]. On the other hand, the developed pattern is largely determined by the nonlinearity in the problem and therefore its length scale may also substantially deviate from the relevant scales of the linearized theory.

A particularly gratifying feature of our variational approach to pattern formation in the normal field instability in magnetic fluids is the possibility to include the wave number modulus k into the set of parameters varied to minimize the energy functional. This allows us to directly determine the dependence of the pattern periodicity on the external magnetic field and to investigate the influence of the variation in wave number on the stability of the different patterns.

We therefore investigate in the present section the wave number selection problem for the Rosensweig instability. For simplicity we will consider a magnetic fluid with infinite depth only. As shown in the previous section this is a very good approximation as long as $d>\lambda_{c,\infty}$. We will compare our findings with recent experiments in which this condition is met.

The necessary calculations are similar to those reported in Sec. IV with the only extension that we no longer fix the wave number modulus k in advance but include it into the set of parameters with respect to which the energy is to be minimized.

A typical result is shown in Fig. 9 displaying the maximal surface deflection $\zeta(0, 0)$ and the corresponding wave number k of the patterns. As can be seen from the figure, the wave number of the patterns decreases with increasing supercriticality. This is in particular pronounced for the square pattern and implies that in this case the system may lower its

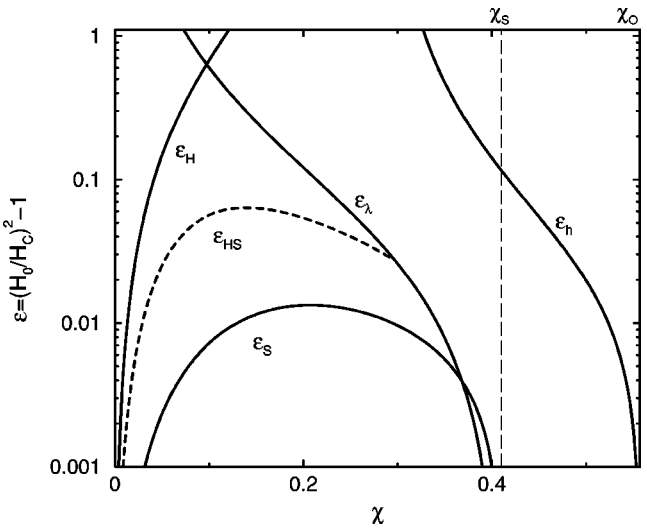

FIG. 10. Limits of the stability regions (solid lines) and Maxwell points (dashed lines) in the χ-ϵ plane if variations of the wave number modulus k are taken into account. Squares are stable if $\epsilon_S<\epsilon<\epsilon_\lambda$. Hexagons are stable if $\epsilon_F<\epsilon<\min(\epsilon_H,\epsilon_h)$. For large values of χ the stability region for squares gets smaller due to the wavelength instability occurring for $\epsilon>\epsilon_\lambda$.

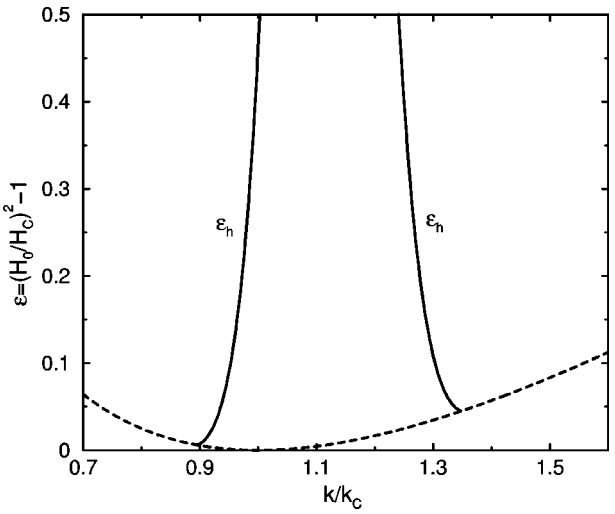

FIG. 11. Stability band of the hexagonal pattern in the k-ϵ plane for a magnetic fluid with $\chi=0.35$. Hexagons become unstable when $\epsilon>\epsilon_h$. The marginal stability curve (dashed line) is also displayed.

energy very efficiently by increasing the wavelength of the pattern.

This effect introduces an additional threshold for ϵ into the stability chart shown in in Fig. 10. If $\epsilon>\epsilon_\lambda$ we find $k\rightarrow 0$ and the pattern disappears by increasing its wavelength to infinity. This process is accompanied by an unbounded increase of the amplitudes A_1, A_4 which carries us outside of the validity of our perturbation *Ansatz* (22). The stability regions of the other pattern remain qualitatively the same as without minimization in k as can be seen from a comparison between Figs. 10 and 4.

For supercritical magnetic fields a whole band of wave numbers giving rise to stable patterns exists. For hexagons this stability region is shown in Fig. 11. At fixed ϵ the hexagonal planform becomes unstable if the wave number is increased sufficiently. In Ref. [4] such an increase of the wave number was achieved experimentally by compressing the hexagonal pattern in a hopper. The observed transition from a hexagonal to a square pattern with smaller wave number occurs when the limit ϵ_h of the stable k band is exceeded and is hence in qualitative agreement with our theory.

VII. DISCUSSION

In the present paper we have theoretically investigated the formation of patterns on the free surface of a magnetic fluid resulting from the Rosensweig instability. For a magnetic fluid layer of arbitrary depth d in an external magnetic field $\mathbf{H}_0$ the equilibrium surface profile was determined by minimizing the appropriate thermodynamic potential. We have assumed a linear dependence of the magnetization on the magnetic field which is at most 5% off the correct values for the experimentally situations with which we compare our findings. The analysis is restricted to the vicinity of the critical magnetic field at which the flat interface becomes unstable since it uses a perturbation expansion for the energy up to fourth order in the amplitude of the surface deflection. Our findings generalize the classical results of Gailitis [7] and Kuznetsov and Spektor [8] to layers of finite depth $d<\infty$.

We have found that, at least for the slightly supercritical magnetic fields considered, the finite thickness of the magnetic fluid layer can be neglected as long as it remains larger than the critical wavelength of the linear instability which in typical experiments is about 1 cm. For thinner layers nonlinear effects become increasingly important. This shows up quite generally in more pronounced hysteresis effects for the transition between different planforms. We also find smaller values of the susceptibilities for which squares and ridges may appear through backward bifurcations and correspondingly higher order terms in the energy are necessary to saturate the instabilities. The critical values of the susceptibility χ beyond which our theory breaks down are displayed in Fig. 6. Together with the findings shown in Fig. 3 they quantify the qualitative statement $\chi\ll 1$ used in Refs. [7] and [8]. An extension of our analysis including higher orders similar to what has been done in Ref. [23] for the one-dimensional situation seems feasible but rather tedious.

It is possible to understand the enhanced hysteretic behavior for thin layers qualitatively. A thin layer inhibits surface deformations resulting from the Rosensweig instability (see Fig. 5) since the magnetic field energy is suppressed due to the finite depth of the layer. On the other hand for the developed pattern the magnetic flux is concentrated at the peaks of the surface so that the effective layer depth becomes larger. Correspondingly the pattern is additionally stabilized and decays only after a reduction of the field stronger than expected from the linear theory. A similar reasoning explains why backward bifurcations of ridges and squares are facilitated in thin layers.

In addition to determining the stable planforms by minimizing the energy functional in the amplitudes of the different modes present in our ansatz for the surface profile, we have also addressed the problem of wave number selection by including the wave number modulus k into the set of variational parameters. We found quite generally a decrease of the wave number of the pattern with increasing magnetic field. This is in qualitative agreement with recent experiments by Abou *et al.* [4] in which the the field intensity was abruptly increased to overcritical values and the corresponding wavelength $\lambda=2\pi/k$ of the resulting hexagonal pattern was found to increase with increasing field. Likewise it was found that the wave number k of the hexagonal pattern is already for slightly supercritical magnetic fields smaller then the critical wave number k_c. The corresponding difference Δk is also found in the theory and shown in Fig. 9. Unfortunately a quantitative comparison with the experimental results is impossible since in the experiment a magnetic fluid with a susceptibility of $1.4>\chi_H$ was used. For such a susceptibility the theoretical analysis would require higher order terms in the perturbation expansion of the energy. Nevertheless we found that Δk grows with increasing susceptibility such that the experimentally observed value of a few percent agrees well with our result for Δk at smaller susceptibilities $\chi<\chi_H$.

Moreover, the theoretical analysis has shown that when including the wave number into the set of variational param-

eters the square pattern gets rather susceptible to an unbounded increase in the wave number. This gives rise to a reduced stability domain for squares and may be related to the fact that in the experiments using jumps in the field intensity always hexagonal arrays of peaks were found [4]. Quite generally our results verify that the resulting planform may depend on the details of the experimentally chosen way to reach overcritical magnetic fields.

Let us finally stress that the variation of the wave number of the patterns with the external field as found here theoretically and observed in the experiments does not invalidate our ansatz with a fixed wave number used before. As reported in Ref. [4] the wave number of the arising hexagonal pattern coincides with k_c if the magnetic field is increased and decreased in a quasistatic way. This is probably due to the fact that the boundary conditions suppress the emergence or disappearance of peaks in a developed pattern. Therefore using the quasistatic process a metastable pattern with k_c is produced whereas a jump in field intensity gives rise to the most stable pattern corresponding to a smaller wave number.

ACKNOWLEDGMENTS

We would like to thank Bérengère Abou for explaining her experimental findings to us and Adrian Lange for interesting discussions. This work was supported by the *Deutsche Forschungsgemeinschaft* under the project En 278/2-1.

[1] M. D. Cowley and R. E. Rosensweig, J. Fluid Mech. **30**, 671 (1967).
[2] R. E. Rosensweig, *Ferrohydrodynamics* (Cambridge University Press, Cambridge, 1985).
[3] D. Allais and J.-E. Wesfreid, Bull. Soc. Fr. Phys. Suppl. **57**, 20 (1985).
[4] B. Abou, J.-E. Wesfreid, and S. Roux, J. Fluid Mech. **416**, 217 (2000).
[5] M. C. Cross and P. H. Hohenberg, Rev. Mod. Phys. **65**, 851 (1993).
[6] A. C. Newell and J. A. Whitehead, J. Fluid Mech. **38**, 279 (1969).
[7] A. Gailitis, J. Fluid Mech. **82**, 401 (1977).
[8] E. A. Kuznetsov and M. D. Spektor, Zh. Eksp. Teor. Fiz. **71**, 262 (1976) [Sov. Phys. JETP **44**, 136 (1976)].
[9] E. E. Twombley and J. W. Thomas, SIAM (Soc. Ind. Appl. Math.) J. Math. Anal. **14**, 736 (1983).
[10] M. Silber and E. Knobloch, Physica D **30**, 83 (1988).
[11] H. Herrero, C. Pérez-Garcìa, and M. Bestehorn, Chaos **4**, 15 (1994).
[12] C. Ku' strup, H. Herrero, and C. Pérez-Garcìa, Phys. Rev. E **54**, 1560 (1996).
[13] B. Abou, G. Néron de Surgy, and J.-E. Wesfreid, J. Phys. II **7**, 1159 (1997).
[14] A. Lange, B. Reimann, and R. Richter, Phys. Rev. E **61**, 5528 (2000).
[15] H. W. Müller, Phys. Rev. E **58**, 6199 (1998).
[16] L. D. Landau and E. M. Lifshitz, *Elektrodynamik der Kontinua* (Akademie-Verlag, Berlin, 1974).
[17] J.-C. Bacri and D. Salin, J. Phys. (France) Lett. **45**, L-559 (1984).
[18] A. G. Boudouvis, J. L. Puchalla, L. E. Scriven, and R. E. Rosensweig, J. Magn. Magn. Mater. **65**, 307 (1987).
[19] V. N. Zaitsev and M. I. Shliomis, Dokl. Akad. Nauk (SSSR) **188**, 1261 (1969) [Sov. Phys. Dokl. **14**, 1001 (1970)].
[20] S. Ciliberto, P. Coullet, J. Lega, E. Pampaloni, and C. Perez-Garcia, Phys. Rev. Lett. **65**, 2370 (1990).
[21] J. Weilepp and H. R. Brand, J. Phys. II **6**, 419 (1996).
[22] R. Bajaj and S. K. Malik, J. Magn. Magn. Mater. **149**, 158 (1995).
[23] A. Engel, H. Langer, and V. Chetverikov, J. Magn. Magn. Mater. **195**, 212 (1999).